ION MOVEMENT THROUGH GRAMICIDIN A CHANNELS

Single-Channel Measurements at Very High Potentials

OLAF SPARRE ANDERSEN

Department of Physiology and Biophysics, Cornell University Medical College, New York, New York 10021

ABSTRACT   The patch-clamp technique of Mueller (1975, *Ann. N. Y. Acad. Sci.*, 274:247–264) and Neher and Sakmann (1976, *Nature (Lond.)*, 260:799–802) was modified to be suitable for single-channel measurements in lipid bilayers at potentials up to 500 mV. This method was used to study gramicidin A single-channel current-voltage characteristics. It was found that the sublinear current-voltage behavior normally observed at low permeant ion concentrations and rather low potentials ($V \leq 200$ mV) continues to be seen all the way up to 500 mV. This phenomenon is characteristic of the low permeant ion situation in which the channel is far from saturation, and implies that the overall rate constant for association between ion and channel is very weakly, if at all, voltage dependent. The magnitude of the single channel currents at 500 mV is consistent with the notion that the aqueous convergence conductance is a significant factor in determining the permeability characteristics of the gramicidin A channel.

INTRODUCTION

Channels formed in lipid bilayer membranes by the polypeptide antibiotic gramicidin A have in recent years played an increasingly important role as a prototype transmembrane channel (for surveys of the literature see Bamberg et al., 1978; Hladky et al., 1979; Hägglund et al., 1979; Andersen and Procopio, 1980; Finkelstein and Andersen, 1981). Gramicidin A has attracted this wide attention for several reasons. First, the experimental accessibility of the gramicidin A channel makes it possible to obtain information about its permeability properties over a very wide range of permeant ion concentrations or applied potentials. It is, therefore, possible to obtain better insight into the biophysical processes underlying the conduction mechanism(s) for this channel than for most other channels. Second, the relatively simple structure (Sarges and Witkopf, 1965 *a, b*) and the existence of a reasonable molecular model for the transmembrane channel (Urry, 1971) promise that it ultimately should be possible to account for the permeability behavior in terms of the molecular structure of the channel. Third, the ideal selectivity of the channel for monovalent cations (Myers and Haydon, 1972; Urban et al., 1980), its selectivity among small monovalent cations (Mueller and Rudin, 1967; Myers and Haydon, 1972; Eisenmann et al., 1976), and the existence of single-file flux-coupling effects (Schagina et al., 1978; Procopio and Andersen, 1979), are all factors that make studies on

gramicidin A channels relevant for understanding the behavior of ion-conducting channels in biological membranes.

Many different experimental techniques have been used to elucidate the permeability characteristics of gramicidin A channels. Single- and many-channel current-voltage measurements have been particularly popular, partly due to their relative simplicity and partly because analysis of the shape of the current-voltage characteristics as a function of permeant ion concentration in principle yields information about the energy profile for ion movement through the channel. Such analyses are fairly model dependent, however, as there is considerable interdependence among any assumptions (and conclusions) made about the height and shape of the energy barriers and the number and positions of coordination sites that can be simultaneously occupied by ions (cf., Eisenman et al., 1980 and Urban et al., 1980). The analysis of current-voltage characteristics, and other ion permeability experiments, will likewise depend upon assumptions made concerning the importance (or lack of importance) of limitations to ion movement imposed by the aqueous convergence regions, whether or not the rate constant for ion movement from the bulk aqueous phase up to the channel entrance is comparable to the rate constant for association between ion and channel.

The impetus for the present investigations was that gramicidin A single-channel currents observed at low permeant ion concentrations and high potentials seemed to reach voltage-independent limiting values, and that the magnitude of these currents was consistent with an aque-

ous convergence (diffusion) resistance limiting the current flow (Andersen, 1978). This conclusion was in apparent conflict with the theoretical analysis of diffusion-limited ion movement through membrane-bound channels by Läuger (1976). But the conflict could not be resolved with conventional single-channel technqiues due to the difficulties in obtaining sufficient data at high potentials. The patch-clamp technique of Mueller (1975) and Neher and Sakmann (1976) was therefore modified to be suitable for single-channel measurements at high potentials ($V \geq 200$ mV).

This article (one of three) presents the experimental technique for single-channel measurements at high potentials, and a discussion of its validity. The main experimental results are that at high potentials the rate constant of association between the channel and a permeating ion is very weakly voltage dependent, and that the magnitude of the single-channel currents at 500 mV is indeed consistent with diffusion-limited ion entry into the channel. The second article (Andersen, 1983 a) considers the origin of the remaining voltage dependence observed at low permeant ion concentrations and high potentials. It will be shown that this voltage dependence is an artifact, arising from the interfacial polarization associated with charging the membrane capacitance. The third article (Andersen, 1983 b) contains the main results of this series of articles: that the aqueous convergence regions are very important factors in determining the permeability properties of gramicidin A channels.

Some of this material has appeared in preliminary form (Andersen and Procopio, 1978, 1980).

MATERIALS AND METHODS

Planar black lipid membranes were formed by the pipet technique of Szabo et al. (1969) across a hole (1.6 mm^2 area) in a Teflon partition separating two Teflon chambers containing the appropriate electrolyte solution. The membrane-forming solutions were either diphytanoylphosphatidylcholine (DPhPC) dissolved in n-decane, 2.0–3.0% wt/vol, or glycerolmonooleate (GMO) dissolved in n-decane, 12.5% wt/vol. The electrolyte solutions were unbuffered (pH $\approx$ 5.5–6) and made up fresh every day. The conductivity of the solutions was measured with a conductivity meter (Model CDM 2, Radiometer, Copenhagen, Denmark). The temperature was generally 25°C. It was maintained constant within 0.5°C, using water circulating in an external jacket. In extreme cases there could be temperature variations as large as 1.0°C from the preset temperature. No corrections were made for these variations in temperature. Gramicidin A was usually added to the aqueous phases before the membranes were formed in order to minimize the time necessary to establish a reasonably constant single-channel activity (membrane conductance). Further additions of gramicidin A were sometimes made during the experiments to maintain the channel activity at a reasonably high level. The nominal concentration of gramicidin A varied between 10^{-12} M and 10^{-11} M. The concentration of ethanol never exceeded 0.5% by volume, a concentration that has no apparent effect upon the single-channel behavior (data not shown).

Single-Channel Measurements

The single-channel current-voltage characteristics were measured using a modification of the glass micropipet or patch-clamp technique (Mueller,
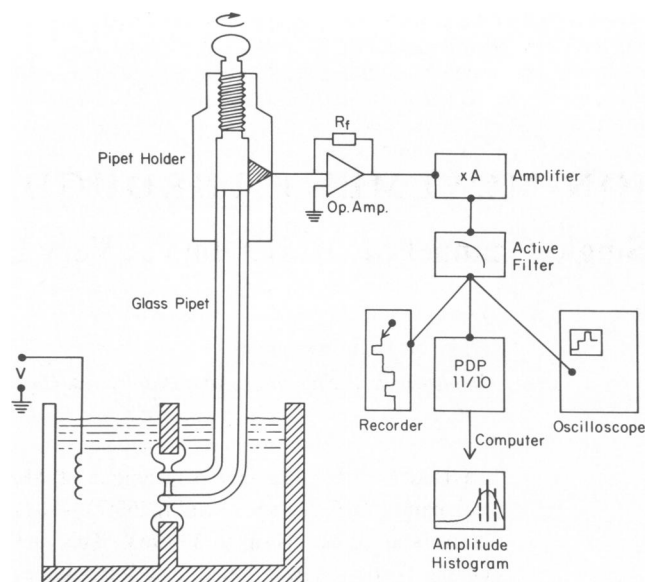

FIGURE 1 Schematic representation of the experimental setup for the single-channel measurements (not drawn to scale). The chamber, micropipet, and current-measuring amplifier are all in a Faraday cage mounted on an air-suspended table. The signal from the cage is amplified, filtered, and continuously displayed on an oscilloscope. Permanent records may be obtained as photographs from the oscilloscope, from the stripchart recorder, and from the computer.

1975; Neher and Sakmann, 1976; Neher et al., 1978 a).[1] Fig. 1 summarizes the experimental setup.

Glass micropipets were pulled by hand in a gas flame from pyrex capillaries with an outer diameter of 0.8 mm and an inner diameter of 0.5 mm. The pipets were cut with a diamond knife and nicked to achieve a right circular break at a point where the outer diameter is between 50 and 300 μm. These pipets were then placed in a microforge, with the platinum filament carefully coated with soft (sodalime) glass to minimize the deposition of a platinum film upon the pipet. A right-angle bend was made ~4 mm from the tip of the pipet and the tip was firepolished to achieve a final inner diameter of 10–40 μm, for experiments with DPhPC, or 40–80 μm for experiments with GMO. The pipet tip was silanized in the microforge under visual control with trioctylsilane undiluted, or as a 10% solution in benzene. Before use, the micropipet was cleaned in chloroform:methanol (2:1 vol/vol), ethanol, and water. It was then mounted in a microelectrode holder (Model 2 HR, W-P Instruments, Inc., New Haven, CT), where the top part was fitted with nylon screw to permit volume changes in the pipet. The assembled pipet and holder was then filled with the electrolyte solution.

The electrical measurements were in all cases made with Ag/AgCl electrodes. The electrode in the front chamber was connected to a voltage source. The electrode in the back chamber was a Ag/AgCl pellet in the microelectrode holder. The plug of the microelectrode holder was inserted into a Teflon-isolated jack which, via a 10^4 Ω guard resistor, was connected to the inverting input of a high input impedance, ultra–low-bias current operational amplifier (AD 515 HL, Analog Devices, Inc., Norwalk, MA) in the virtual-ground mode. The feedback resistance of the current-measuring amplifier was 10^9 or 10^{10} Ω. The current-measuring amplifier was built into a small shielded box mounted upon a micromanipulator. The output from the amplifier was amplified (10–10,000 times) with a preamplifier, and filtered with a four-pole Bessel filter to achieve

---

optimal noise reduction, while maintaining the shape of the current transitions with minimal distortion. The cutoff frequency determined by the filter setting was the -8.6 dB frequency. To minimize the pickup of electrical or mechanical noise, the experiments were done in a mechanically solid Faraday cage mounted upon an air-suspended table (Servabench, Mark IVC, Barry-Wright Corp., Watertown, MA).

Before the measurements began, it was ensured that there was electrical contact between the two electrodes (the resistance through the pipet varied with the electrolyte concentration, the total resistance varied between 10^5 Ω and 10^7 Ω), and that they were in balance (the imbalance was <0.5 mV; this was regularly checked every two to four measurements). A large bilayer was then formed across the hole in the Teflon partition and the glass micropipet was pushed through the colored part of a thick membrane to coat it with an excess of lipid. The pipet could then be pushed through the bilayer itself without breaking it. This allowed for the isolation of bilayers with areas of 10^{-6} to 10^{-5} cm^2, and sometimes less. Fig. 2 A and B illustrate the process in more detail. With this system it was possible to record single-channel current transitions with an amplitude $<2.5 \times 10^{-14}$ A using a 10^{10} Ω feedback resistor (Fig. 2 C). In 1.0 M salt the background conductances were generally ~1 pS, although higher values certainly were observed. The intrinsic noise of the measuring system (amplifier plus feedback resistor) at low frequencies domi-

nated the thermal noise from the feedback resistor; only a little additional noise was introduced by the external voltage source and the pipet (plus membrane). In addition to good performance with respect to electrical and mechanical noise, this system also gave excellent membrane stability at very high applied potentials, as the small membranes could last for minutes with 500 mV applied (data not shown). In exceptional cases, potentials as high as 600 mV could be applied and several single-channel transitions could be observed. The lifetimes of the small membranes varied with the applied potential, from a few milliseconds to several hours.

The single-channel current transitions were analyzed on-line by a

FIGURE 3 The data-collecting scheme. A single channel is drawn schematically in the top part. The bar at right illustrates the discrimination level; its magnitude is determined by looking at the channels on the oscilloscope screen. The digitized record corresponding to this channel is illustrated in the bottom part. The digitized data are transiently stored in a circular buffer in the computer memory. Two successive points (denoted by arrows) differ by more than the discrimination level at the channel opening and at the channel closing. Each of these events trigger the data-collection routine. Beginning with the last data point before the discrimination level was exceeded, the computer searches a fixed number N ($5 \leq N \leq 10$) points back in the buffer. If these all differ by less than the discrimination level, the pretransition current level is termed well-defined and its value is obtained as the average value of the N points (illustrated by the thin horizontal line). The posttransition level is then determined. The point at which the discrimination level was exceeded and the next are disregarded. The next N points are then used to determine whether the level is well defined. If both levels are well defined the current transition is called well defined. The value of the posttransition current level is again evaluated, as the average value of the N points, and the height of the current transition is determined as the absolute value of the difference between the posttransition level and the pretransition level.
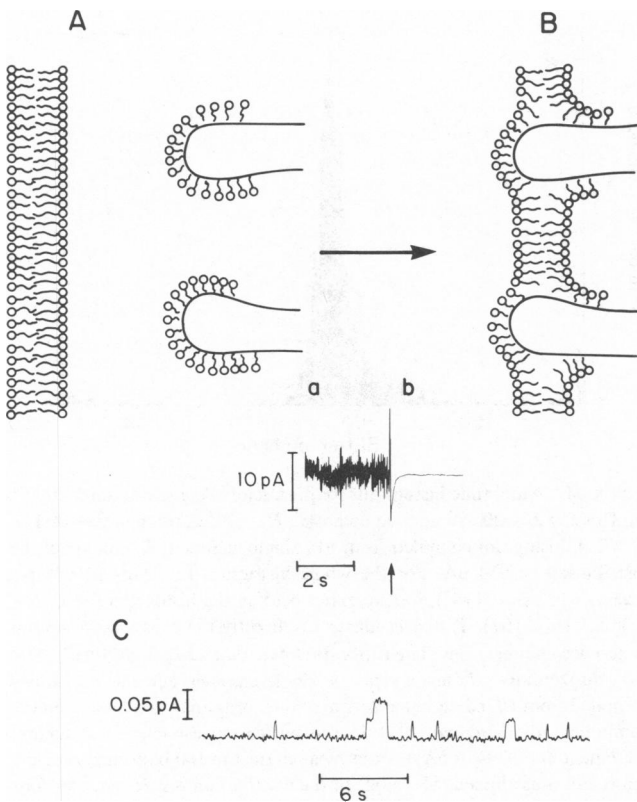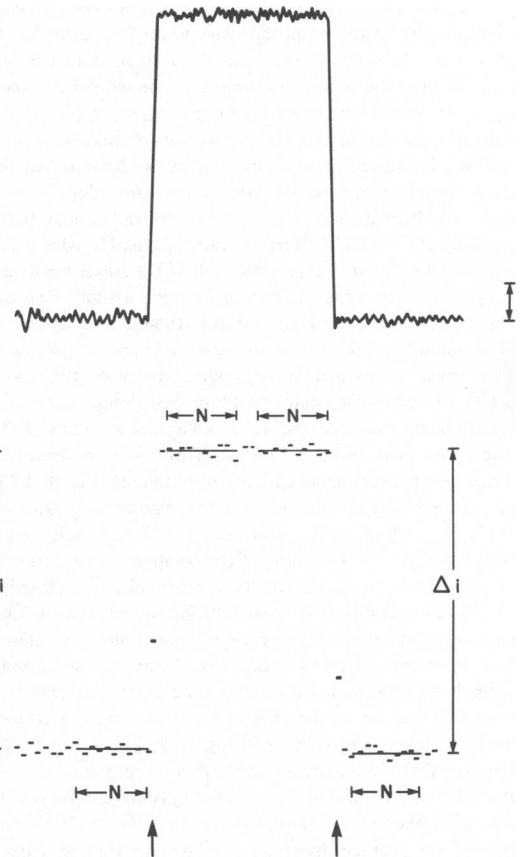

FIGURE 2 The formation of a small membrane. The top part illustrates the membrane events, the bottom part illustrates the electrical correlates. The arrows denote the formation. (*A*) The pipet is in the back chamber behind the large membrane. (*a*) The corresponding noise trace. (*B*) The pipet has been pushed through the large membrane, and the pipet opening is now occluded by a small segment of the original bilayer — the small membrane. (*b*) The electrical noise decreases drastically commensurate with the membrane formation (the decrease in capacitance). DPhPC, 1.0M NaCl, $T = 25°C$, $R_f = 10^{10}$ Ω, filter = 100 Hz. (*C*) Electrical performance of the system. A stripchart record of gramicidin A channels at high resolution. DPhPC, 0.1 M LiCl + 0.4 M TEACl in D$_2$O, 25°C, $R_f = 10^{10}$ Ω.

laboratory minicomputer (PDP 11/10, Digital Equipment Corp., Maynard, MA). The incoming voltage signal was digitized at a rate determined by the settings of the filter (sampling interval $= 1/[2 \cdot$ frequency]). Discrete voltage transitions were recognized when two points differed by more than a preset discrimination level (1.5–2 times the peak-to-peak base-line noise). This triggered the actual data sampling routine written by Daniel T. Brown to be linked into Dan Brown Basic, and the initial and final voltage levels were stored for subsequent analysis (see Fig. 3 for more detail). The average value of the current transitions for a given experiment was obtained immediately following the experiment. The computer displayed the absolute differences between initial and final voltages for all well-defined transitions in an amplitude histogram. The mean current and the standard deviation were then calculated for the major peak in the amplitude histogram (see below). The final determination of the single-channel current (mean, standard deviation) was calculated from the values determined for the individual experiments weighted by the number of transitions in each experiment.

A composite histogram, based upon all the experiments in 0.1 M RbCl at 300 mV used for the final data evaluation, is illustrated in Fig. 4. A manually collected histogram of part of the same data is shown for comparison. The histogram is characterized by five features: (a) a major peak consisting of 65–95% of all transitions (labeled II), which represents the most common channel type observed; (b) a small peak near zero (labeled 0), caused by channels lasting for such a short time that they trigger the pattern-recognition routine even though the current level has returned to the initial level by the time the levels are actually calculated; (c) a small peak positioned at approximately twice the major peak (labeled III), caused by the almost simultaneous opening or closing of two channels; (d) a small and somewhat variable peak located slightly to the left of the major peak (labeled I), caused by the existence of a rather well-defined group of channels with an amplitude that is 70–80% of the amplitude of the major population — such a channel is illustrated in the *inset* of Fig. 4; and (e) a few scattered transitions that, in part, are artifacts produced by the switching of the computer to and from the rest of the equipment, e.g., when the small bilayer breaks or in other instances when a new small membrane is formed during the data collection period. Only the major population (II) of channel transitions is of interest here. The other contributions to the amplitude histogram were noted and ignored. Such an exclusion can be done in a fairly consistent manner. Table I summarizes the results obtained with each of the 10 individual measurements used to construct the histogram in Fig. 4. The analysis can be done in a consistent manner, and the long-term reproducibility is good.[2] The major effect of "trimming" the histogram is to decrease the standard deviations, while the mean values of the currents are little affected. The mean value of the average single-channel currents changes from 2.69 ± 0.08 pA (mean ± SD, $n = 10$) for the raw data to 2.69 ± 0.05 pA for the intermediate step, where the events corresponding to populations 0 and III are excluded, to 2.74 ± 0.05 pA for the final data, which also exclude population I. The single-channel currents estimated this way are similar to the currents estimated from the mode of the amplitude histogram (see Table I). The difference between the two methods of estimating the single-channel currents is statistically insignificant ($\bar{i}_m - \bar{i} = 0.001 \pm 0.029$ pA (mean ± SD, $n = 10$).

Many-Channel Experiments

These were double-pulse experiments, using a conventional two-electrode voltage-clamp setup (Andersen and Fuchs, 1975). The current traces

were recorded with a digital oscilloscope (Explorer III, Nicolet Instrument Co., Milwaukee, WI) and stored on minidiskettes for later analysis. The voltage-dependence of the current was determined as the ratio of current during a test pulse to the current at the reference potential in the same composite pulse. The $R \cdot C$ time constant for charging the membrane
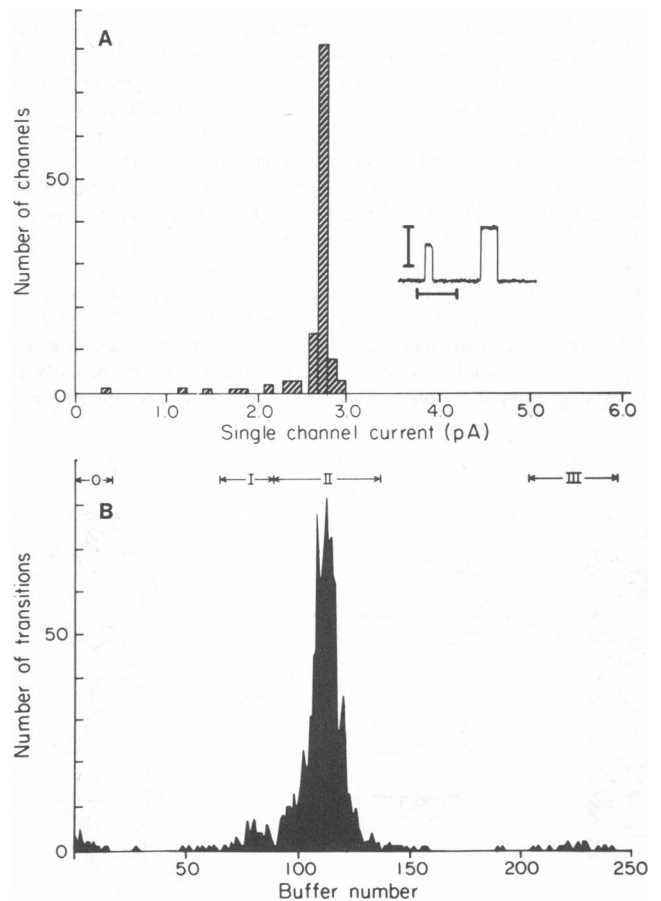

FIGURE 4 Amplitude histograms for gramicidin A single channels in 0.1 M, RbCl, with 300 mV applied potential, $R_f = 10^9 \, \Omega$, filter $= 50$–100 Hz, 25°C. *A*, histogram compiled from 119 single channels. The mode of the distribution is 2.74 pA. For the whole histogram $\bar{i} = 2.66 \pm 0.34$ pA [mean ± SD ($n = 119$)], for the major peak in the histogram $\bar{i} = 2.75 \pm 0.05$ pA ($n = 107$). The *inset* illustrates directly the existence of several difference channel sizes. The calibration bars denote 2pA, vertically, and 1 s, horizontally. *B*, histograms of single-channel current transitions compiled from 10 individual experimental records analyzed on-line on the computer. An increment of 1 in the buffer corresponds to a current increment of 0.024414 pA, the abscissae in the top and bottom part of the figure are thus aligned. The mode of the distribution is 2.76 pA. The four regions, labeled *0, I, II, III*, illustrate the most conspicuous aspects of the histograms. *0* denotes current transitions where the data acquisition routine was triggered by a brief spike, such that the current returned to the base-line before the second level was to be determined. *I* denotes a population of channels with an amplitude less than the most commonly seen amplitude (see the *inset* in the top part of the diagram). *II* denotes the major population of channels. *III* denotes a small number of events where two channels opened simultaneously within the time-resolution determined by the filter setting. For the whole histogram $\bar{i} = 2.74 \pm 0.58$ pA ($n = 1257$). For the major population, *II*, $\bar{i} = 2.75 \pm 0.18$ pA ($n = 1130$), for population *III*, $\bar{i} = 5.50 \pm 0.23$ pA ($n = 21$), and for population *I*, $\bar{i} = 1.99 \pm 0.13$ pA ($n = 61$). The standard deviations are larger than for the manually compiled histogram. This is instrumental, as the mean square deviation from zero in population *0*, is 0.15 pA ($n = 21$).

[2]It was occasionally observed that the average current for the first one or two experiments with a pipet was systematically larger (by 25% or even higher) than the remaining data at that potential. This was particularly noticeable if the applied potential was negative (relative to the pipet). Such results were checked by additional measurements at that potential (generally a total of eight independent determinations) or in exceptional cases where the deviations exceeded 50% or so, the result from the first determination was disregarded.

TABLE I
ANALYSIS OF SINGLE-CHANNEL CURRENTS

| | | Experiment number | | | | | | | | | |
		78-05 11-7	78-05 11-8	78-05 11-26	78-05 11-27	78-05 12-1	78-05 12-2	79-04 17-1	79-04 17-2	79-04 17-10	79-04 17-11
Raw data	$\bar{i}$	2.63	2.64	2.75	2.61	2.74	2.60	2.64	2.79	2.68	2.82
	SD	0.74	0.56	0.28	0.31	0.50	0.45	0.91	0.58	0.38	0.81
	n	69	109	95	114	126	108	109	174	230	123
Intermediate	$\bar{i}$	2.74	2.62	2.75	2.63	2.71	2.64	2.68	2.76	2.69	2.69
step	SD	0.15	0.28	0.28	0.20	0.22	0.30	0.38	0.29	0.24	0.31
	n	64	105	95	113	123	106	97	168	227	113
Final data	$\bar{i}$	2.77	2.71	2.81	2.66	2.73	2.68	2.73	2.81	2.74	2.80
	SD	0.12	0.13	0.13	0.12	0.19	0.25	0.12	0.15	0.12	0.10
	n	61	87	84	105	120	101	79	147	204	86
Mode	$\bar{i}_m$	2.78	2.69	2.86	2.66	2.69	2.69	2.76	2.83	2.73	2.76

DPhPC membranes, $V = 300$ mV, $T = 25°C$, $R_f = 10^9 \, \Omega$, filter = 50–100 Hz.
"Raw data" represents the complete histogram for each measurement; "intermediate step" denotes the result after exclusion of population 0 and III; "final data" denotes the results from the major peak; "mode" denotes the most frequent current transition in the complete histogram.

capacitance was ~1.7 μs. It was therefore possible to measure the gramicidin A–induced currents accurately ~20 μs after applying the test pulse. (The gramicidin A–induced currents were kept <30 μA, while the peak of the initial capacitative current spike could be 2,000 μA. A systematic error <1% in the current reading became possible only after ~12 time constants.) It was necessary to guard against artifacts rising from current variations due to electrostriction phenomena (Benz and Janko, 1976) or voltage-induced conductance relaxations (Bamberg and Läuger, 1973). The currents were therefore checked to see if they remained constant (within 1%) for at least 25 μs after the completion of the capacitative transient during the test pulse, and to see if they returned to the pretest level when the potential was returned to the reference level. This was found to be the case for experiments with GMO membranes, but not for DPPC membranes at high potentials (see Results).

Materials and Cleaning Procedures

Standard cleaning of the chambers consisted of successive rinses in water, ethanol, and chloroform:methanol (2:1 vol/vol); this was done twice. This rinsing effectively removes lipids and the gramicidin A. After a few days of use, the chambers were taken apart and cleaned in ethanolic NaOH during sonication. This procedure was followed by repeated sonications in water, acetone, chloroform:methanol (2:1 vol/vol) and petroleum ether.

Pyrex capillaries (redrawn tubing) were obtained from Corning Glass Works (Corning, NY). They were cleaned by boiling in 6 M HCl and then sonicating; this was done twice. They were then cleaned by sonication, three times in deionized H_2O and three times in chloroform:methanol (2:1 vol/vol). Trioctylsilane was obtained from Pfalz & Bauer, Inc. (Stamford, CT) or from Petrarch Systems (Levittown, PA).

Diphytanoylphosphatidylcholine was obtained from Avanti Polar Lipids (Birmingham, AL). It gave a single spot on thin-layer chromatograms. To ensure that experiments at low ionic strengths would not be overly biased by surface potential effects due to fixed surface charges, the lipid was further cleaned by ion exchange chromatography using a modification of the method of Rouser et al. (1967). The resulting material had zeta potentials ranging between -2 and 0 mV in 10 mM NaCl,[3] and gave a single spot on thin-layer chromatograms. Glycerolmonooleate was obtained from Sigma Chemical Co. (St. Louis, MO) was used without

further purification. Decane was either reference substance for gas chromatography obtained from E. Merck, Darmstadt (through MCB, Cincinnati, OH) or 99.9% pure from Wiley Organics (Columbus, OH). Both were used without further purification.

Gramicidin A was a generous gift from the late Lyman C. Craig of The Rockefeller University. The preparation was presumably a mixture of valine and isoleucine gramicidin A, but it should otherwise have been free of any impurities.
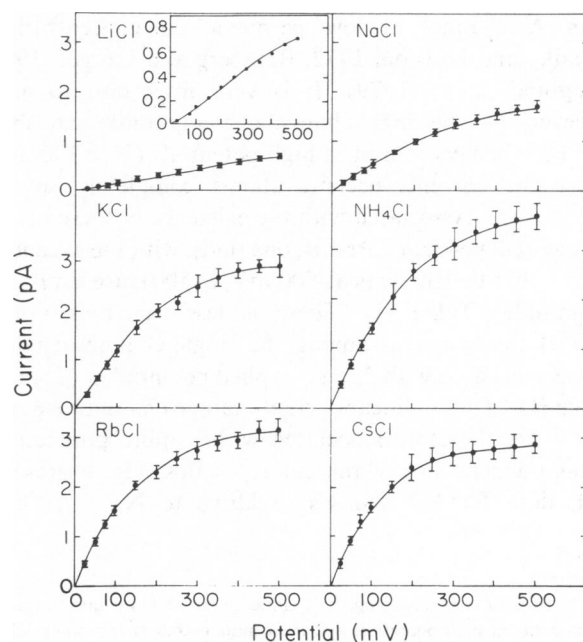

FIGURE 5 Gramicidin A single-channel current-voltage characteristics at low permeant ion concentrations. Each point indicates the mean ($\pm$ SD) of the current. To facilitate visual comparison of different records, they are all drawn to the same scale (except for the *inset* illustrating the LiCl data at a 3.25 × magnification). The solid lines are drawn by hand. 0.1 M salt, DPhPC, 25°C.

---

[3] I would like to thank Dr. S. G. A. McLaughlin for this measurement.

The inorganic salts were either AR grade from Fisher Scientific Co. (Pittsburgh, PA) (LiCl, NaCl, KCl), Analar grade (AR) from British Drug Houses (through Gallard-Schlesinger, Carle Place, NY) (KCl, RbCl, CsCl), or Suprapur grade from E. Merck (through MCB) (LiCl, NaCl, RbCl, CsCl, NH₄Cl). All alkali metal ion salts were roasted for at least 24 h at 550–650°C and stored in evacuated dessicators over NaOH. Tetraethylammonium chloride (TEACl) and tetramethylammonium chloride (obtained from Eastman Kodak Co., Rochester, NY) was recrystallized once from ethanol and acetone and stored over NaOH in an evacuated dessicator. The resulting material gave colorless solutions at 1 M and contained $<0.02\%$ NH_4^+ or similar permeant impurities. Sucrose was density gradient grade from Beckman Instruments, Inc. (Palo Alto, CA), glycerol was spectroscopic quality from Fisher, and urea was ultrapure grade from Schwarz Mann Div. Kratos, Inc. (Spring Valley, NY).

The water was deionized Millipore Corp. Milli-Q water (Bedford, MA); the D_2O was Gold Label, 99.8% D, from Aldrich Chemical Co., Inc. (Milwaukee, WI).

RESULTS

Single-Channel Measurements

Current-Voltage Characteristics and Conductance Ratios in Diphytanoylphosphatidylcholine Membranes. Fig. 5 illustrates gramidicin A single-channel current-voltage characteristics obtained with low aqueous concentrations of the alkali metal cations and NH_4^+ (0.1 M, as chloride salts). At low potentials ($V \leq 200$ mV) the shape of the current-voltage characteristics is sublinear; i.e., the single-channel currents tend to level off towards the voltage axis (except for Li^+, the least permeant ion). This seems to be a characteristic property of the gramicidin A channel at low permeant-ion concentrations (Hladky and Haydon, 1972; Bamberg and Läuger, 1977; Hägglund et al., 1979). It is very important to note, however, that the single-channel currents continue to show sublinear behavior, even at high potentials ($V > 300$ mV) where the currents become almost completely voltage independent. Associated with the existence of these nearly voltage-independent currents, one finds, with the exception of Li^+, that the currents at 500 mV, i (500), are similar in magnitude (Table II). There is less variation among i (500) than there is among the single-channel conductances measured with 25 mV applied potential, g (25) (see Table II).[4] The sublinear current-voltage characteristics in Fig. 5 are therefore associated with a quite pronounced voltage dependence of the current ratios. Fig. 6 presents such data for K^+ and Cs^+ relative to Na^+. At high

---

[4]The reason for characterizing the channel permeability properties using the currents at high potentials and the conductances at low potentials is that they both provide a measure of the unidirectional ion flux through the channel. At sufficiently high potentials ($V \geq 120$ mV) the currents are proportional to the unidirectional ion fluxes, while the small-signal conductance, g, in the absence of isotope interactions is related to the unidirectional ion fluxes at equilibrium, J, by $g = e^2 \cdot J/kT$ (e is the elementary charge, k is Boltzmann's constant, and T is temperature in Kelvin).

TABLE II
GRAMICIDIN A SINGLE-CONDUCTANCES AND CURRENTS

	Units	Li^+	Na^+	K^+	Rb^+	Cs^+	NH_4^+
$g(25)$	pS	1.38	5.17	12.7	18.1	18.0	17.8
SD		0.29	0.95	1.6	1.8	1.7	1.9
g^*_{max}	pS	14.0	33.3	56.1	61.2	55.7	76.2
$g(25)/g_{max}$		0.099	0.16	0.23	0.30	0.32	0.23
$i(500)$	pA	0.72	1.71	2.88	3.14	2.86	3.91
SD		0.05	0.12	0.24	0.25	0.18	0.27
$D\ddagger (\times 10^5)$	cm^2/s	1.03	1.33	1.95	2.07	2.05	1.96
$r_0\S$	Å	0.12	0.21	0.24	0.25	0.23	0.33

0.1 M (as chloride salts), DPhPC, 25°C. Mean and standard deviation.
*g_{max} denotes the maximal single channel conductance, in 0.1 M salt, as calculated using Eq. 3 (see Discussion).
‡D denotes the aqueous diffusion coefficient for the ions, as calculated from Robinson and Stokes (1965, Appendix Table 6.2)
§r_0 denotes the capture radius, as calculated using Eq. 1 (see Discussion).

potentials the conductance ratios approach the ratio of the aqueous diffusion coefficients for the ions.

The sublinear current-voltage characteristics obtained at low permeant ion concentrations (Fig. 5) differ strikingly from the current-voltage characteristics at high concentrations (e.g., 2.0 M) of the same permeant ions (Fig. 7). The shape is superlinear, i.e., the single-channel currents bend toward the current axis. The currents are
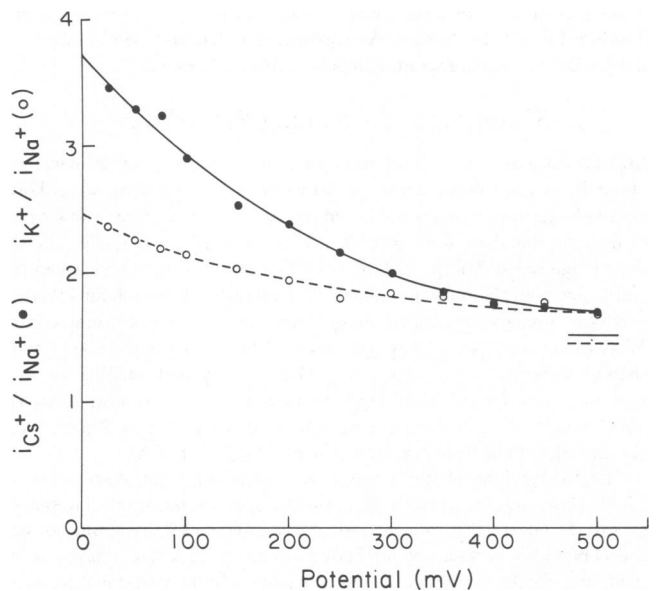

FIGURE 6 Gramicidin A single-channel current ratios as a function of applied potential ● indicates i_{Cs^+}/i_{Na^+}, the points are connected by the solid curve. The solid line in the right-most part of the diagram denotes the ratio of the aqueous diffusion coefficients. ○ indicates i_{K^+}/i_{Na^+}, the points are connected by the interrupted curve. The interrupted line to the right denotes the ratio of the aqueous diffusion coefficient. 0.1 M salt; DPhPC, 25°C.
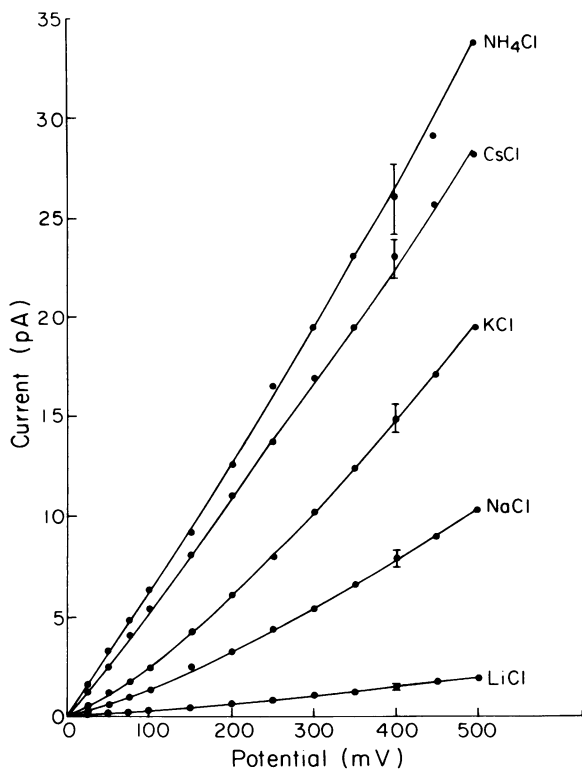
FIGURE 7 Gramicidin A single-channel current-voltage characteristics at high permeant ion concentrations. Each point indicates the mean value of the current. The 400 mV point also denotes the standard deviations. (The data for Rb^+ are essentially super-imposable on the Cs^+ data and are not illustrated.) The solid curves are drawn by hand. 2.0 M salt; DPhPC, 25°C.

much larger in magnitude and they vary more with the type of permeant ion. The shift in the shape of the current-voltage characteristics, from sublinear at low permeant ion concentrations to superlinear at high concentrations reflects a shift of the rate-determining step for ion translocation through the channel (Hladky and Haydon, 1972). Because this shift is associated with a large increase in the single-channel conductance, one may conclude that the sublinear current-voltage characteristics observed at high potentials and at low permeant-ion concentrations reflect the kinetics of ion entry into the gramicidin A channel (see Discussion).

Current-Voltage Characteristics in Glycerol-monooleate Membranes. Fig. 8 illustrates gramicidin A single-channel current-voltage characteristics obtained with gramicidin A channels in GMO membranes. The permeant ions are, again, the alkali metal cations and NH_4^+ (0.1 M, as chloride salts). Table III summarizes the values for g (25) and i (500). The shapes of the current-voltage characteristics are similar to those obtained in DPhPC membranes, i.e., they are sublinear at low potentials and continue to be sublinear at very high potentials. The trend towards a voltage-independent limiting current is less pronounced, however. This is, in part, due to
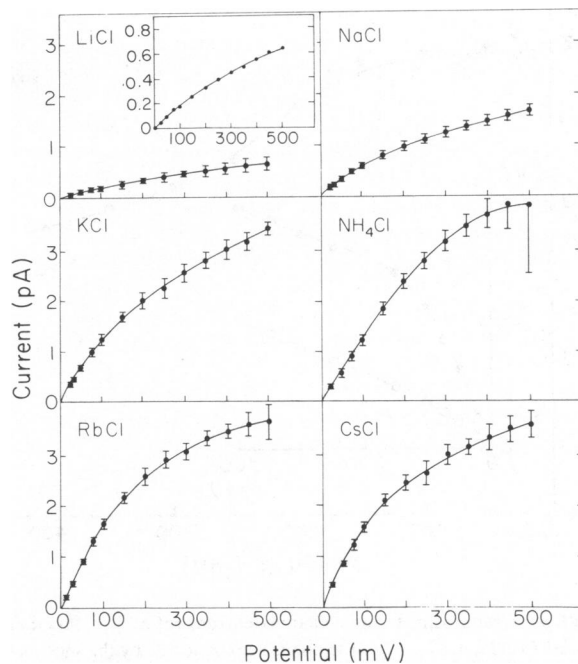

FIGURE 8 Gramicidin A single-channel current-voltage characteristics. Each point indicates the mean (± SD) of the current. (The exceptionally large scatter of the data with 0.1 M NH_4Cl, at 500 mV reflects the diffculty of the measurement. Only 43 transitions were collected.) To facilitate the visual comparison of different records, they are all drawn to the same scale (except for the *inset* illustrating the LiCl data at a 3.25 × magnification). The solid curves are drawn by hand. 0.1 M salt; GMO, 25°C.

interfacial polarization effects associated with having a large potential difference across the membrane (Andersen, 1983 a; see also Discussion), but other effects may also play a role. The voltage dependence of the current ratios in 0.1 M salt is, for example, much less pronounced for channels in GMO membranes than for channels in DPhPC membranes (data not shown). This is not, however, a general characteristic, because at lower salt concentrations (e.g., 0.01 M) the current ratios in GMO membranes retain a voltage dependence qualitatively similar to that observed in DPhPC membranes (Fig. 9). Note that the current ratios below 100 mV are almost indistinguishable from the permeability ratios determined by Urban et al. (1980) from biionic potential measurements (the signifi-

TABLE III
GRAMICIDIN A SINGLE-CHANNEL CONDUCTANCES AND CURRENTS IN GMO MEMBRANES

	Units	Li^+	Na^+	K^+	Rb^+	Cs^+	NH_4^+
$g(25)$	pS	1.89	6.95	14.0	18.7	17.6	11.6
SD		0.23	1.28	2.0	1.7	2.1	1.4
$i(500)$	pA	0.629	1.66	3.44	3.66	3.59	3.91
SD		0.116	0.11	0.13	0.34	0.28	1.36

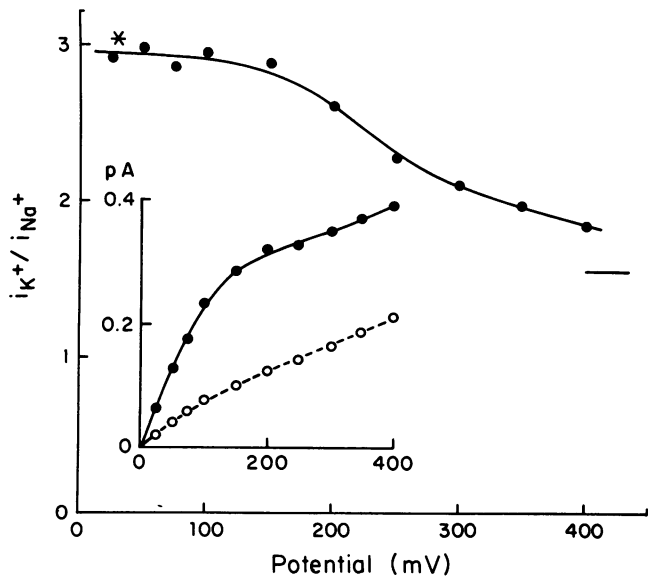0.1 M (as chloride salts), 25°C.
Mean and standard deviation.

FIGURE 9 Gramicidin A single-channel current ratios as a function of potential. O indicates i_{K^+}/i_{Na^+}, the points are connected by the solid curve. The solid line in the right-most part of the diagram denotes the ratio of the aqueous diffusion coefficients. The * indicates the permeability ratio from biionic potential measurements (Urban et al., 1980). Inset: The single-channel current-voltage characteristics used to calculate the current ratios. ● denotes data in KCl, the points are connected by the solid line. O denotes data in NaCl, the points are connected by the interrupted line. 0.01 M salt; GMO, 25°C.

FIGURE 11 Comparison of normalized conductance-voltage characteristics from many-channel membranes and single-channel experiments. ● indicates mean (± SD) of the normalized conductance $[G(V)/G (25)]$ from four membranes modified with many gramicidin A channels. The reference potential was 25 mV. The small-signal conductance varied between from 3×10^{-3} to 1.3×10^{-2} S/cm². × indicates $g(V)/g (25)$ from single-channel experiment (Andersen, 1983 b). The solid line was drawn by hand. 0.1 M CsCl + 0.4 M TEACl; GMO, 25°C. Inset: Current trace from a composite pulse experiment where the reference potential was 25 mV and the test potential, 400 mV, was applied ~300 μs into the pulse. The calibration bars denote 10 μA (vertically) and 200 μs (horizontally). Membrane area, 1.49 mm².

cance of this finding will be discussed in Andersen, 1983 b). This concentration dependence of the shape of the current ratio vs. potential curves suggests that gramicidin A channels in GMO membranes are more affected by ion occupancy effects than channels in DPhPC membranes (as would be the case if the dissociation constants for ion binding into channels in GMO membranes are less than for ion binding into channels in DPhPC membranes).

The Single-Channel Currents Show No Time Dependence. The inset in Fig. 4 indicates that the single-channel open-close events are "clean"; i.e., there is no evidence of transients (slow openings or overshoots) in
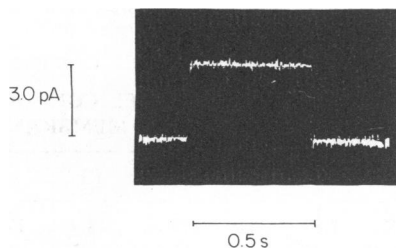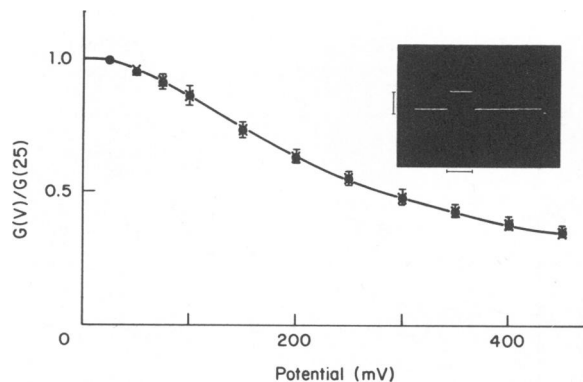

FIGURE 10 Gramicidin A channel recorded at high resolution. Note rectangular shape, essentially constant noise, and absence of an initial overshoot or other irregular behavior. 0.1 M KCl + 0.4 M TEACl, DPhPC, 450 mV, $R_f = 10^9$ Ω, filter = 160 Hz, 25°C.

the records or channel instabilities (multistate behavior) at these high potentials. Fig. 10 shows an oscillographic recording of a single-channel open-close event at better time resolution. The current shows no transient responses within the available time resolution (10–90% rise time ~4 ms), and the magnitude of the current noise is not visibly changed when the channel opens or closes.

Many-Channel Experiments

Experiments were also done on large membranes (up to 1.5 mm² in area) with a high density of gramicidin A channels. It is in this case possible to examine the voltage dependence of the instantaneous currents, and compare this information with the voltage-dependence of the single-channel currents.

Fig. 11 inset illustrates a current trace observed in a GMO membrane, after a test potential of 375 mV was applied on top of a 25 mV reference potential (the total applied potential was 400 mV). The current trace is flat from 25 μs out to 200 μs after applying the test pulse, and the current returns to the pretest level upon return to the reference potential. There is no evidence for voltage-induced current relaxations during this time period. The normalized conductance of the many-channel membrane has the same voltage dependence as in the single channel experiments (Fig. 11). The clean current trace and the identity of the voltage dependencies make it unlikely that there are major, slow, voltage-dependent alterations in channel structure. This is important, because such structural relaxations would probably affect the shape (and thus
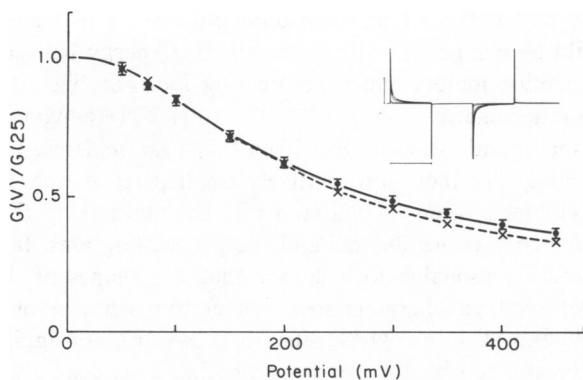
FIGURE 12 Comparison of normalized conductance-voltage characteristics from many-channel membranes and single-channel experiments. ● indicates mean (± SD) of the normalized conductance $[G(V)/G\,(25)]$ from four membranes modified with many gramicidin A channels. The test pulse was 1 ms long, and the record was read at towards the end of the pulse to minimize admixture of electrostrictive currents. The reference potential was 25 mV. The small-signal conductance varied between 3.7×10^{-3} and $2.5 \times 10^{-2}\,S/cm^2$. × indicates $g(V)/g\,(25)$ from single-channel experiments (Andersen, 1983 b). 0.1 M CsCl + 0.4 M TEACl; DPhPC, 25°C. Inset: Current traces recorded from an unmodified DPhPC bilayer. The voltage pulses were 2 ms long at 100, 200, 300, 400, and 500 mV, respectively. Note how the current traces at 100 and 200 mV are essentially clean and confluent, apart from the initial capacitance transient, while there are significant additional current relaxations at higher potentials. (Note also how the current traces are clean when V returns to 0). The calibration bars denote 25 μA (vertically) and 2 ms (horizontally). Membrane area, 1.51 mm^2.

the interpretation) of the single-channel current-voltage characteristics (Läuger et al., 1980).

Similar measurements were also attempted in DPhPC membranes. In this situation, however, it was not possible to achieve satisfactory records, as the current recordings at high potentials were confounded by very large electrostrictive current transients through the unmodified membrane (Fig. 12 inset). The shapes of many-channel conductance-potential characteristics will consequently differ from the shapes of the corresponding single-channel characteristics. The extent of the differences becomes more pronounced as the potential increases (Fig. 12).

DISCUSSION

In sections 1 and 2, I discuss of the validity of single-channel current-voltage characteristics at the high potential used in these studies. Section 3 is a brief discussion of a problem that arises in the analysis of the current-voltage characteristics: that the applied potential will polarize the membrane-solution interfaces. Section 4 contains a discussion of the major result in this article: that ion entry into the gramicidin A channel at very high potentials is almost completely voltage-independent, at least for the most permeant ions (K^+, Rb^+, Cs^+, and NH_4^+). It will also be shown that the magnitude of the currents at these very high

potentials qualitatively is consistent with the notion that ion entry into the gramicidin A channel is diffusion controlled.

Experimental Limitations of Single-Channel Measurements at High Potentials

Steady-state single-channel current measurements at high (>300 mV) potentials are limited by the breakdown of the bilayer. This comes about in two ways: First, the membranes may not last long enough to provide satisfactory data. Second, the membrane may give rise to irregular conductance fluctuations that are not associated with the opening or closing of single gramicidin A channels (see for example, Yafuso et al., 1974).

The first limitation may be overcome by working with very small membrane areas. The breakdown of a lipid bilayer is probably not a process that occurs uniformly over the whole membrane surface. More likely it originates in one or more discrete regions of the bilayer, from which it spreads and ultimately breaks the membrane. The probability of breakdown will thus depend upon the membrane area, the magnitude of the applied potential, the duration for which the potential is applied and the presence of impurities in the lipid or in the aqueous solution. (Gallagher, 1975, especially section 3.10, should be consulted for discussion of statistical theories of dielectric breakdown). A decrease in membrane area should increase the average lifetime of the membranes. The decrease in area was accomplished with the pipet method, and was indeed associated with an increase in membrane stability, as large bilayers generally broke instantaneously if a potential of 300 mV or greater was accidentally applied across them.

The second limitation was overcome by ensuring that the current transitions to be used in the analysis were between levels that lasted longer than a predetermined time, at least five sampling points (15 to 300 ms, depending upon filter setting), and by ensuring that the level was constant within preset limits, usually 1.5–2.0 times the peak-to-peak base-line noise. These two criteria assure that the computer only accepts discrete stepwise changes in membrane currents to signify that a channel opens or closes. The criteria used in the computer-aided analysis are thus very similar to those used when analyzing a stripchart record of single-channel activity. This does not guarantee that a particular transition is due to the opening or closing of a Gramicidin A channel, but it should assure that a population of transitions with a very similar magnitude represents the opening and closing events of gramicidin A channels with a minimal contamination of junk (i.e., extraneous and infrequent current steps).

A comparison with gramicidin A single-channel conductance values obtained by other workers (Hladky and Haydon, 1972; Neher et al., 1978 b; Apell et al., 1979;

Urban et al., 1980) shows that the present results are in agreement with those in the literature. One can, in particular, compare the small-signal conductances in GMO membranes (Table III) with the data in Table I of Neher et al. (1978 b) and Table VIII of Urban et al. (1980). The rather small deviations ($\leq 12\%$) can be accounted for by differences in temperature and by the different potentials used in the different series of experiments.

The shapes of the single-channel current-voltage characteristics in GMO membranes (see Fig. 8) are in agreement with those obtained by others (Hladky and Haydon, 1972; Hladky, 1974 a; Urban et al., 1980), but they differ from the shapes of the many-channel characteristics reported by Bamberg and Läuger (1977) and Hägglund et al. (1979). The present data show a more pronounced sublinear behavior. The reason for these discrepancies is not entirely clear, as the many-channel conductance-voltage characteristic reported here for GMO is in good agreement with the single-channel conductance-voltage data (see Fig. 11). But it seems likely that any discrepancies that may exist between single-channel data and many-channel data reflect imperfections in the latter, due to the existence of additional (electrostrictive) current transitions (see Fig. 12, *inset*). These contributions to the total membrane current produce an upward shift in the conductance-voltage relations (Fig. 12).

The Channel May Be Regarded as a Stable Structure

The close similarity between the many-channel current-voltage characteristics and the single-channel current-voltage characteristics (see Figs. 11 and 12), taken together with the rectangular shape of the single-channel current transitions (Fig. 10) indicates that these data reflect the behavior of the channel as a fairly stable structure or, more likely, as a structure that fluctuates very rapidly between a number of states. In the latter case one may regard the channel as having a "fixed" structure with properties determined by the time average of the properties of the different states (Läuger et al., 1980). That is, if the current-voltage characteristics in part reflect voltage-dependent transitions between several conducting states of the channel, this will be reflected in the magnitude and voltage dependence of the rate constants for translocation through the time-averaged channel structure.

It is, in particular, important to note that the effects of the applied field itself upon the channel should be trivial compared with the interactions between the permeating ions and the channel. At 500 mV applied potential the field is $\sim 2 \times 10^6$ V/cm. This is a large field, but the interaction energy of this field with an aligned peptide (HN—C=O) moiety having a dipole moment of ~ 3.6 D Debye (estimated from dipole moments for low-molecular weight amides in McClellan, 1963) is nevertheless moderate, 2.4

$\times 10^{-21}$ J (~ 0.6 kT at room temperature).[5] This energy should be compared with the interaction energy between the peptide moiety and a permeating ion. For Na^+ this interaction energy is $\sim 4 \times 10^{-19}$ J (~ 100 kT) (Renugopalakrishnan and Urry, 1978).[6] Even the large fields used in this study are therefore relatively small perturbations of the channel, when compared with the interactions that occur between the channel and the permeating ions. It is therefore reasonable to conclude that the shapes of the current-voltage characteristics reflect the behavior of a conducting structure whose intrinsic behavior is not significantly affected by the applied potential. This conclusion will be amplified in the next article (Andersen, 1983 a).

Interfacial Polarization Effects

The single-channel currents observed at low permeant ion concentrations and very high potentials show a small but finite voltage dependent (Figs. 5 and 8). This voltage dependence is a consequence of the fact that the channel is incorporated into a lipid bilayer structure with a finite capacitance. That is, the current-voltage characteristics of the gramicidin A channels are affected by interfacial polarization or ion injection effects, similar to those described by Walz et al. (1969).

The origin of this interfacial polarization is that the membrane capacitance must be charged when a potential difference is applied across a bilayer. This charging process is associated with an accumulation of cations and depletion of anions at the positive membrane-solution interface (and vice versa at the negative interface). The increase in the interfacial cation concentration at the positive interface will, of course, affect any process limited by the rate of cation association with a membrane-bound structure, and it becomes in principle impossible to observe a voltage-independent limiting current (Andersen, 1983 a).

The Association Step is Essentially Voltage Independent and May Be Diffusion Controlled

Ion movement through a narrow (single-filing) channel involves five distinct steps: (a) diffusion through the aque-

---

[5]The overall interaction of the field on the channel will, of course, be summed over all the peptide moieties, where the neighboring peptide groups are antiparallel to one another in the β_6-helical dimer (Urry, 1971). The total interaction energy between the channel and the field should thus be considerably less than the sum of the absolute interaction energies. It is, however, in this respect important to consider the extent that the behavior of one peptide group is coupled to that of its neighbors.
[6]The calculation of this interaction energy is complex, as emphasized by the authors. The quoted value is therefore subject to some uncertainty, mainly due to the large electrostatic field variations close to the ion. This means that the interaction energy depends upon the detailed charge distribution in the peptide moiety, and considerable uncertainty seems to exist with regards to this latter question (Hagler and Lapiccerella, 1976; Lifson et al., 1979).

ous phases up to the channel; (b) association with the channel entrance; (c) translocation through the channel interior; (d) dissociation from the channel; and (e) diffusion through the aqueous phases out from the channel. The shape of the single-channel current-voltage characteristics will depend upon the relative magnitude of the resistances (barrier heights) imposed by each step, as well as the voltage dependence for ion movement across the associated barrier. Concentration-dependent variations in the shape of current-voltage characteristics must thus reflect concentration-dependent variations in the relative magnitude of the resistances imposed by the various steps.

Different combinations of resistances (barrier heights) and voltage dependences may combine to produce sublinear current-voltage characteristics at low potentials and permeant ion concentrations. A particular important case is that of a fast and fairly voltage-dependent translocation through the channel interior combined with a slow and relatively voltage-independent dissociation step (Hladky and Haydon, 1972; Läuger, 1973; Hladky et al., 1979; Hägglund, Eisenman, and Sandblom, in preparation). Sublinear behavior at high potentials will, on the other hand, primarily reflect the characteristics of the association reaction(s) (see the Appendix for a more extensive discussion).

Current-voltage characteristics that possess voltage-independent currents at high potentials can, in general, be associated with one of four different mechanisms (Fig. 13). First, the entry step into the channel may be voltage independent; i.e., if there is no spatial barrier associated with the entry step (such that there is no potential drop across the barrier) or, more likely, if no barrier is associated with the entry step. Second, the exit step could be voltage independent. Third, ion movement through the channel could be limited by the (voltage-independent) movement of water molecules in a single-filing channel operating in the vacancy mode, or some other voltage-independent process with first-order kinetics. Finally, ion movement may be limited by diffusion through the aqueous phases up to the channel.

A voltage-independent exit step can be excluded by noting that the single-channel current-voltage characteristics change shape, from downward concave to convex, when the permeant ion concentration is increased and the resistance imposed by the association step is decreased (compare Figs. 5 and 7). This is associated with an increase in the relative resistance imposed by the channel itself (that is, everything except the association step) and with an increase in ion occupancy in the channel. The single-channel currents at high salt concentrations are therefore limited by the rate of ion movement through the channel and, in particular, out of the channel. A voltage-independent exit step should thus be more important at high concentrations, when the currents become concentration independent. But the voltage dependence became more pronounced at high concentrations; the exit step must therefore be voltage dependent. A similar argument can be used to exclude other mechanisms with first-order kinetics, i.e., any steps subsequent to the association between ion and channel (unless there is a drastic concentration dependent variation in the voltage-dependence of one or more steps). It can thus be shown that single-file flux coupling between ions and water cannot be the barrier. Therefore, I conclude that the current-voltage characteristics observed at low permeant-ion concentrations reflect the kinetics of ions entering the channels, at least at high potentials.

A comparison of the results in Fig. 5 with the theoretical current-voltage characteristics in Fig. 14 (see the Appendix) shows that the overall voltage-dependence of the association step is quite small in DPhPC membranes. (1.7 $\pm$ 0.6% [mean $\pm$ SD] of the applied potential seems to affect the association step [data for K^+, Rb^+, Cs^+, and NH_4^+, 300 mV $\le V \le$ 500 mV].) This residual voltage dependence is primarily a reflection of interfacial polarization effects (Andersen, 1983 a). Somewhat larger voltage dependence of the currents at high potentials is seen with channels in GMO membranes (Fig. 8), where 6 $\pm$ 2% of the potential seems to affect the association step. This large voltage dependence is, at least in part, a reflection of interfacial polarization effects, because addition of 0.4 M TEACl to 0.1 M salt of a permeant ion decreases the voltage dependence to 2 $\pm$ 1% (data from Andersen, 1983 b, Fig. 4), but direct effects of ion occupany are presumably also important, because the voltage variation in the single channel current ratios is concentration dependent in the 0.01 $-$ 0.1 M concentration range. It is reasonable to conclude that the intrinsic voltage dependence of the association reaction at very high potentials is small, also in GMO membranes. This conclusion is consistent with that of Eisenman et al. (1980).

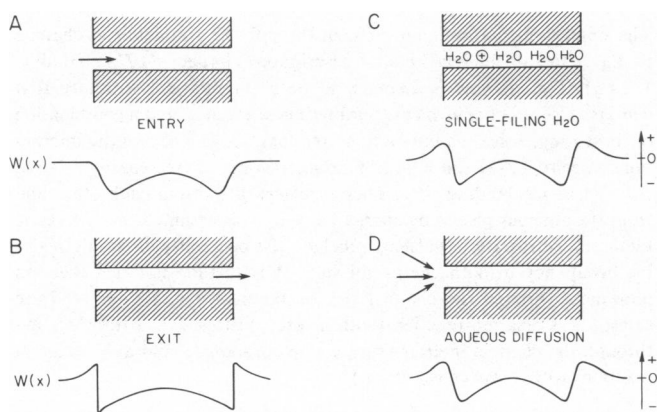The behavior of the single-channel currents at high

FIGURE 13 Schematic illustration of the four possible mechanisms that will produce voltage-independent limiting currents in single-channel current-voltage measurements. $W(x)$ denotes the free energy for an ion as it traverses the channel.

potentials is qualitatively consistent with the pattern expected for diffusion-limited ion movement up to the channel entrance. The currents are nearly independent of potential (except for Li^+ and to some extent Na^+), and the magnitudes of i (500) are in reasonable agreement with the predictions of the first-order theory of diffusion-controlled ion movement up to the channel entrance (see below). Factors other than diffusion limitations are important, however, in determining the overall permeability characteristics of the channel, because the current increments seen at potentials above 100 mV are much larger than predicted for a purely diffusion-controlled process (compare Figs. 5 and 8 with Fig. 14 or, better, Fig. 9 of Andersen, 1983 a). An appreciable resistance to ion movement must therefore reside in the channel, either because the height of the energy barriers produces a significant resistance or because ion occupancy (saturation effects) in the channel has increased its resistance. Both factors are likely to be important, but their relative importance cannot be assessed without detailed information about the kinetics of ion movement through the channel.

The magnitude of a diffusion-controlled currents, i_D, is determined by the size and geometry of the channel entrance, by the aqueous diffusion coefficient, D, and the permeant ion concentration, c (Läuger, 1976):

$$i_D = F \cdot f \cdot r_o \cdot D \cdot c \qquad (1)^7$$

where F is Faraday's constant, f is a factor that depends on the particular geometry assumed for the channel entrance ($f = 2 \cdot \pi$ if the entrance is a hemisphere), and r_o is the capture radius for the ion and reflects the difference between channel radius and ion radius (Ferry, 1936). A rough estimate for i_D is obtained by setting $r_o = 1$ Å, $D = 10^{-5}$ cm^2/s. For $c = 0.1$ M, one thus finds that i_D should be ~6 pA, which is in reasonable agreement with the measured i (500). The diffusion-controlled current is equal to the uni-directional current through the aqueous convergence regions at zero potential. Information about i_D thus provides the means to estimate the small-signal conductance of the aqueous convergence region, g_a:

$$g_a = e \cdot i_D/kT \qquad (2)$$

where e is the elementary charge, k is Boltzman's constant, and T is temperature in Kelvin. When the intrinsic channel conductance becomes infinitely large, the measured channel conductance will approach its maximal value, g_{max}:

$$g_{max} = g_a/2 = e \cdot i_D/(2 \cdot kT). \qquad (3)$$

---

[7]The voltage-independent limiting current can be up to two times larger than i_D because the electrical field in the convergence region may give rise to an electromigrative component to the current (Läuger, 1976). This contribution is, however, negligible in the present case because the electroneutrality assumption fails to apply in the convergence region (Andersen, manuscript in preparation.)
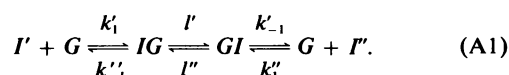
If it is assumed that i (500) $\approx i_D$ then r_o and g_{max} can be estimated, see Table II. (These estimates will be ~30% too high because interfacial polarization effects are neglected. Similar calculations are not presented for the data in Table III because the larger voltage dependence of the currents at high potentials makes the assumption that i (500) $\approx i_D$ dubious. The values of i (500) in Tables II and III show, however, a general similarity). The data in Table II show two important features. First, g (25) and g_{max} are close to each other, g (25)/g_{max} varies between 0.1 for Li^+ and 0.3 for Cs^+. The former value is underestimated, but the ratios for K^+, Rb^+, Cs^+, and NH_4^+, and probably also for Na^+, should be reasonably correct. Second, the magnitude for r_o is reasonable for a diffusion-controlled current considering that r_o is a parameter that describes the critical dimensions involved in the movement of particles with radii between 0.5 and 1.6 Å (the ion crystal radii, Hille, 1975) through a channel with a 2 Å radius (Urry, 1972).

The values estimated for r_o argue that diffusion limitations should be seriously considered as a factor affecting the rate of ion movement through the channel. The large values found for g (25)/g_{max} suggest further that diffusion limitations may be important for the small-signal (near-equilibrium) properties of the channel, at least at low permeant ion concentrations. To demonstrate that diffusion limitations indeed are important, two requirements must be met. Firstly, it must be shown that the single-channel currents at sufficiently high potentials become intrinsically voltage independent. This will be done in the second article in this series (Andersen, 1983 a). Secondly, it must be shown that the currents at high potentials vary appropriately with changes in the bulk aqueous phase diffusion coefficients of the permeant ions. This will be done in the third article in this series (Andersen, 1983 b).

APPENDIX

Sublinear Current-Voltage Characteristics

The simplest model for ion movement through the gramicidin A channel is the two-site-one-ion kinetic description (Läuger, 1973; Hladky, 1974 a). The channel is assumed to be a symmetrical structure that contains a series of equivalent coordination sites, such that a combination of short-range solvation interactions and long-range electrostatic interactions (Levitt, 1978) combine to produce two major free energy minima that act as ion binding sites. These are separated from each other and from the aqueous phases by energy barriers. It is assumed that energetic factors (electrostatic repulsion) preclude the possibility of simultaneous ion occupancy in both energy minima. It is further assumed that ion movement through the channel can be subdivided into three separate steps, an association reaction (with a rate constant k_1), a translocation through the channel interior (with a rate constant l), and a dissociation reaction (with a rate constant k_{-1}):

$$I' + G \underset{k'_{-1}}{\overset{k'_1}{\rightleftharpoons}} IG \underset{l''}{\overset{l'}{\rightleftharpoons}} GI \underset{k''_1}{\overset{k'_{-1}}{\rightleftharpoons}} G + I''. \qquad (A1)$$

I' and I'' represent an ion in the left and right aqueous phases, respectively. G, IG, and GI denote a gramicidin A channel without ions, or with ion the

left or the right free energy minimum (site). The superscripts ' and " for the rate constants denote that their magnitudes will be biased by the applied potential: At zero potential no bias exists and the superscripts can be dropped. In symmetrical aqueous phases the current through the channel is:

$$i(u) = \frac{2 \cdot e \cdot k_1 \cdot l \cdot k_{-1} \cdot c \cdot \sinh(u/2)/S(u)}{(k'_{-1} \cdot k''_{-1} + k'_{-1} \cdot l' + k''_{-1} \cdot l'')} \\ + c[(k'_1 + k''_1) \cdot (l' + l'') + k'_{-1} \cdot k'_1 + k''_{-1} \cdot k''_1]$$ (A2)

where c is the permeant ion concentration, $S(u)$ is a "shape function" whose form depends upon the details of the barrier shapes (Hall et al., 1973; Hladky, 1974 b; Andersen and Fuchs, 1975), and u is the dimensionless potential:

$$u = V \cdot e/kT.$$ (A3)

If the barriers are sharp, such that the dependence of the rate constants on potential are exponential functions of the potential difference between a barrier peak and the adjacent well (or aqueous phase), and they are symmetrical, then Eq. A2 condenses to

$$i(u) = e \cdot k_{-1} \cdot l \cdot c \cdot \sinh(u/2)/\mathbf{D}$$ (A4)

where

$$\mathbf{D} = K \cdot \{k_{-1}/2 + l \cdot \cosh[(1 + \delta) \cdot u/4]\}$$
$$+ c \cdot (k_{-1} \cdot \cosh[(1 - \delta) \cdot u/2] +$$
$$l \cdot \{\cosh[(1 - 3\delta) \cdot u/4] + \cosh[(1 + \delta) \cdot u/4]\}).$$ (A5)

$K = k_{-1}/k$ is the single-site dissociation constant and δ is the fraction of the applied potential that falls between the two energy wells (see Fig. 14).

Fig. 14 illustrates the normalized current-voltage characteristics predicted from Eq. A4, for different values of δ when $l = 10 \cdot k_{-1}$ and $c = 0.1 \cdot K$. The current-voltage characteristics are in all cases sublinear at low potentials, but at high potentials ($V > 200$ mV) the current begins to increase as an exponential function of potential, unless $\delta = 1.0$. There are also significant differences among the current-voltage characteristics at
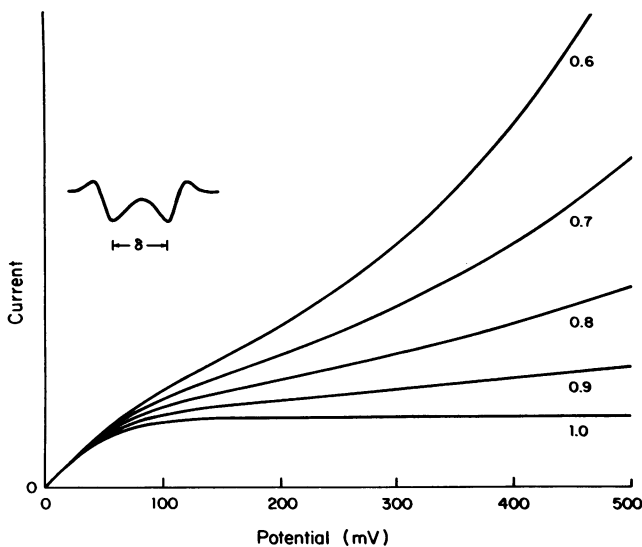

FIGURE 14 Single-channel current-voltage characteristics calculated from Eq. C3. *Inset*: Illustration of the barrier model and of the definition of δ. The numbers close to the different curves denote the different values of δ.

lower potentials. These differences have not been used in the present study, because their interpretation depends upon knowledge (or assumptions made) about the shape function $S(u)$, and because arguments about the existence and importance of the aqueous convergence conductance must be made on the basis of the magnitude of the single-channel currents and how they change with changes in bulk aqueous phase transport characteristics.

The physical basis for the sublinear shape at low potentials, and low permeant ion concentrations, is that ion movement through the channel is limited by ion exit out of the channel when $k_{-1} \ll l$, such that the ion distribution between the two energy minima in the channel is potential dependent and approaches the Boltzmann distribution as $k_{-1}/l \rightarrow 0$. The current is:

$$i(u) = e \cdot [k'_1 \cdot c \cdot W(G) - k''_{-1} \cdot W(IG)]$$ (A6)

where $W(G)$ and $W(IG)$ denote the probability of finding the channel is state G or IG, respectively:

$$W(G) = K \cdot \{k_{-1}/2 + l \cdot \cosh[(1 + \delta)u/4]\}/\mathbf{D}$$ (A7)

$$W(IG) = c \cdot [k_{-1} \cdot \exp((1 - \delta) \cdot u/2) +$$
$$l \cdot \{\exp[(1 - 3\delta) \cdot u/4] + \exp[-(1 + \delta)u/4]\}]/\mathbf{D}.$$ (A8)

An increase in $u(u = u' - u'')$ will, at fairly low potentials ($u \sim 1$), increase the current by increasing k'_1 (unless k_1 is voltage independent, $\delta = 1.0$) and by decreasing k''_{-1} and $W(G)$ (if $c \ll K$ then $W(G)$ will be close to 1 and approximately constant). If $k_{-1} \ll l$, the decrease in $W(IG)$ will be steep function of u (unless $\delta \ll 1$). In this case the initial increase in $i(u)$ reflects primarily the decrease in the $k''_{-1} \cdot W(IG)$ term. But $W(IG)$ can only decrease to zero. (when all ions in the channel are in the right hand energy well). The effects of decreasing $W(IG)$ will therefore rapidly diminish, thus producing the sublinear current-voltage characteristic seen at low potentials. But as u increases further, $i(u)$ enters a new phase of exponential growth (unless $\delta = 1.0$), because the voltage-dependent increase in k'_1 finally manifests itself. It is then possible to study the behavior of the association step. If, for example, the exponential increase in $i(u)$ does not materialize, even at very high potentials, one can conclude that the association reaction is very weakly, if at all, voltage dependent.

The assumption that at most one ion can occupy the channel at any time is invalid at high permeant ion concentrations where at least two ions simultaneously can occupy the gramicidin A channel (Schagina et al., 1978; Procopio and Andersen, 1979; Eisenman et al., 1980; Urban et al., 1980). Multiple (double) ion occupancy will not, however, affect the conclusion, that the magnitude and voltage dependence of single-channel currents measured at very high potentials and low permeant ion concentrations (where the currents are linear functions of the concentration) reflect the characteristics of the association step, at least as long as $k_{-1} \ll l$.

REFERENCES

Andersen, O. S. 1978. Ion transport across simple membranes. *In* Renal Function. G. H. Giebisch and E. F. Purcell, editors. Josiah Macy, Jr. Foundation, New York. 71–99.

Andersen, O. S. 1983 a. Ion movement through gramicidin A channels. Interfacial polarization effects on single-channel current measurements. *Biophys. J.* 41:135–146.

Andersen, O. S. 1983 b. Ion movement through gramicidin A channels. Studies on the diffusion-controlled association step. *Biophys. J.* 41:147–165.

Andersen, O. S., and M. Fuchs. 1975. Potential energy barriers to ion transport within lipid bilayers: studies with tetraphenylborate. *Biophys. J.* 15:795–830.

Andersen, O. S., and J. Procopio. 1978. Ion entry into gramicidin A channels. *Biophys. J.* 21:26 a. (*Abstr.*).

Andersen, O. S., and J. Procopio. 1980. Ion movement through gramicidin A channels. On the importance of the aqueous diffusion resistance and ion-water interactions. *Acta Physiol. Scand. Suppl.* 481:27–35.

Apell, H.-J., E. Bamberg, and P. Läuger. 1979. Effects of surface charge on the conductance of the gramicidin channel. *Biochim. Biophys. Acta.* 552:369–378.

Bamberg, E., and P. Läuger. 1973. Channel formation kinetics of gramicidin A in lipid bilayer membranes. *J. Membr. Biol.* 11:177–194.

Bamberg, E., and P. Läuger. 1977. Blocking of the gramicidin A channel by divalent cations. *J. Membr. Biol.* 35:351–375.

Bamberg, E., H.-J. Apell, H. Alpes, E. Gross, J. L. Morell, I. J. Harbaugh, and P. Läuger. 1978. Ion channels formed by chemical analogs of gramicidin A. *Fed. Proc.* 37:2633–2637.

Benz, R., and K. Janko. 1976. Voltage-induced capacitance relaxation of lipid bilayer membranes. Effects of membrane composition. *Biochim. Biophys. Acta.* 455:721–738.

Eisenman, G., S. Krasne, and S. Ciani. 1976. Further studies on ion selectivity. *In* International Workshop on Ion Selective Electrodes and on Enzyme Electrodes in Biology and in Medicine. M. Kessler, L. Clark, D. Lubbers, I. Silver, and W. Simon, editors. Verlag Urban und Schwarzenberg, Munchen. 3–21.

Eisenman, G., J. Hägglund, J. Sandblom, and B. Enos. 1980. The current-voltage behavior of ion channels: important features of the energy profile of the gramicidin channel deduced from the conductance-voltage characteristics in the limit of low ion concentrations. *Ups. J. Med. Sci.* 85:247–257.

Ferry, J. D. 1936. Statistical evaluation of sieve constants in ultrafiltration. *J. Gen. Physiol.* 20:95–104.

Finkelstein, A., and O. S. Andersen. 1981. The gramicidin A channel: A review of its permeability characteristics with special reference to the single-file aspect of transport. *J. Membr. Biol.* 59:155–171.

Gallagher, T. J. 1975. Simple Dielectric Liquids. Mobility, Conduction and Breakdown. Clarendon Press, Oxford. 120–130.

Hagler, A. T., and A. Lapiccerella. 1976. Spatial electron distribution and population analysis of amides, carboxylic acid, and peptides, and their relation to empirical potential functions. *Biopolymers.* 15:1167–1200.

Hall, J. E., C. A. Mead, and G. Szabo. 1973. A barrier model for current flow in lipid bilayer membranes. *J. Membr. Biol.* 11:75–97.

Hägglund, J., B. Enos, and G. Eisenman. 1979. Multi-site, multi-barrier, multi-occupany models for the electrical behavior of single filing channels like those of gramicidin. *Brain Res. Bull.* 4:154–158.

Hille, B. 1975 a. Ionic selectivity of Na and K channels in nerve membranes. *In* Membranes. Lipid Bilayers and Biological Membranes: Dynamics Properties. G. Eisenman, editor. Marcel Dekker, Inc., New York. 3:255–323.

Hladky, S. B.. 1974 a. Pore or carrier? Gramicidin A as a simple pore. *In* Drugs and Transport Processes. B. A. Callingham, editor. The McMillan Press, Ltd., London. 193–210.

Hladky, S. B. 1974 b. The energy barriers to ion transport by nonactin across thin lipid membranes. *Biochim. Biophys. Acta.* 352:71–85.

Hladky, S. B., and D. A. Haydon. 1972. Ion transfer across lipid membranes in the presence of gramicidin A. Studies of the unit conductance channel. *Biochim. Biophys. Acta.* 274:294–312.

Hladky, S. B., B. W. Urban, and D. A. Haydon. 1979. Ion movements in the gramicidin pore. *In* Membrane Transport Processes. C. F. Stevens and R. W. Tsien, editors. Raven Press, New York. 3:89–103.

Läuger, P. 1973. Ion transport through pores: a rate-theory analysis. *Biochim. Biophys. Acta.* 311:423–441.

Läuger, P. 1976. Diffusion-limited ion flow through pores. *Biochim. Biophys. Acta.* 455:493–509.

Läuger, P., W. Stephan, and E. Frehland. 1980. Fluctuations of barrier structure in ionic channels. *Biochim. Biophys. Acta.* 602:167–180.

Levitt, D. G. 1978. Electrostatic calculations for an ion channel. I. Energy and potential profiles and interactions between ions. *Biophys. J.* 22:209–219.

Lifson, S., A. T. Hagler, and P. Dauber. 1979. Consistent force field studies of intermolecular forces in hydrogen-bounded crystals. I. Carboxylic acids, amides, and the C═O: :H–Hydrogen Bonds. *J. Am. Chem. Soc.* 101:5111–5121.

McClellan, A. L. 1963. Tables of Experimental Dipole Moments. W. H. Freeman & Co., Publishers, San Francisco. 9-566.

Mueller, P. 1975. Membrane excitation through voltage induced aggregation of channel precursors. *Ann. N. Y. Acad. Sci.* 264:247–264.

Mueller, P., and D. O. Rudin. 1967. Development of K^+-Na^+ discrimination in experimental bimolecular lipid membranes by macrocyclic antibiotics. *Biochem. Biophys. Res. Comm.* 26:398–404.

Myers, V. B., and D. A. Haydon. 1972. Ion transfer across lipid membranes in the presence of gramicidin A. II. The ion selectivity. *Biochim. Biophys. Acta.* 274:313–322.

Neher, E., and Sakmann, B. 1976. Single-channel currents recorded from membrane of denervated frog muscle fibers. *Nature (Lond.).* 260:779–802.

Neher, E., B. Sakmann, and J. H. Steinbach. 1978 a. The extracellular patch clamp: a method for resolving currents through individual open channels. *Pflügers Arch. Eur. J. Physiol.* 375:219–228.

Neher, E., J. Sandblom, and G. Eisenman. 1978 b. Ionic selectivity, saturation, and block in gramicidin A channels. II. Saturation behavior of single-channel conductances and evidence for the existence of multiple binding sites in the channel. *J. Membr. Biol.* 40:97–116.

Procopio, J., and O. S. Andersen. 1979. Ion tracer fluxes through gramicidin A modified lipid bilayers. *Biophys. J.* 25(2, Pt. 2):8 a. (*Abstr.*)

Renugopalakrishnan, V., and D. W. Urry. 1978. A theoretical study of Na^+ and Mg^{+2} binding to the carbonyl oxygen of N-methyl acetamide. *Biophys. J.* 24:729–738.

Robinson, R. A., and R. H. Stokes. 1965. Electrolyte Solutions. 2nd edition, revised. Butterworths Co., Ltd., London. 465.

Rouser, G., G. Kritchevsky, and A. Yamamoto. 1967. Column chromatographic and associated procedures for separation and determination of phosphatides and glycolipids. *In* Lipid Chromatographic Analysis. G. V. Mannetti, editor. Marcel Dekker, Inc., New York. 1:99–162.

Sarges, R., and B. Witkop. 1965 a. Gramicidin. V. The structure of valine — and isoleucine-gramicidin A. *J. Am. Chem. Soc.* 87:2011–2020.

Sarges, R., and B. Witkop. 1965 b. Gramicidin A. VI. The synthesis of valine — and isoleucine-gramicidin A. *J. Am. Chem. Soc.* 87:2020–2027.

Schagina, L. V., A. E. Grinfeldt, and A. A. Lev. 1978. Interaction of cation fluxes in gramicidin A channels in lipid bilayer membranes. *Nature (Lond.).* 273:243–245.

Szabo, G., G. Eisenman, and S. Ciani. 1969. The effects of the macrotetralide actin antibiotics on the electrical properties of phospholipid bilayer membranes. *J. Membr. Biol.* 1:346–382.

Urban, B. W., S. B. Hladky, and D. A. Haydon. 1980. Ion movements in gramicidin pores. An example of single-file transport. *Biochim. Biophys. Acta.* 602:331–354.

Urry, D. W. 1971. The gramicidin A transmembrane channel: a proposed (L. D.) helix. *Proc. Natl. Acad. Sci. U. S. A.* 68:672–676.

Urry, D. W. 1972. Protein conformation in biomembranes: optical rotation and absorption of membrane suspensions. *Biochim. Biophys. Acta.* 265:115–168.

Walz, D., E. Bamberg, and P. Läuger. 1969. Nonlinear electrical effects in lipid bilayer membranes. I. Ion injection. *Biophys. J.* 9:1150–1159.

Yafuso, M., S. J. Kennedy, and A. R. Freeman. 1974. Spontaneous conductance changes, multilevel conductance states and negative differential resistance in oxidized cholesterol black lipid membranes. *J. Membr. Biol.* 17:201–212.